



Contents lists available at ScienceDirect

Biochemical Pharmacology

journal homepage: www.elsevier.com/locate/biochempharm

Honokiol induces proteasomal degradation of AML1-ETO oncoprotein via increasing ubiquitin conjugase UbcH8 expression in leukemia

Bin Zhou^{a,1}, Haiying Li^{a,1}, Chongyun Xing^b, Haige Ye^b, Jianhua Feng^b, Jianbo Wu^a, Zhongqiu Lu^c, Jing Fang^d, Shenmeng Gao^{a,*}

^a Laboratory of Internal Medicine, The First Affiliated Hospital of Wenzhou Medical University, Nanbaixiang, Ouhai District, Wenzhou, Zhejiang Province 325000, China

^b Department of Hematology, The First Affiliated Hospital of Wenzhou Medical University, Nanbaixiang, Ouhai District, Wenzhou, Zhejiang Province 325000, China

^c Department of Emergency Medicine, The First Affiliated Hospital of Wenzhou Medical University, Nanbaixiang, Ouhai District, Wenzhou, Zhejiang Province 325000, China

^d Department of Drug Discovery and Biomedical Sciences, South Carolina College of Pharmacy, University of South Carolina, Columbia, SC, USA

ARTICLE INFO

Article history:

Received 6 October 2016

Accepted 28 December 2016

Available online xxx

Chemical compounds studied in this article:

Honokiol (PubChem CID 72303)

Trichostatin A (PubChem CID 444732)

Keywords:

Honokiol

AML1-ETO

UbcH8

ABSTRACT

AML1-ETO is the most common oncoprotein leading to acute myeloid leukemia (AML), in which 5-year survival rate is only about 30%. However, currently there are no specific therapies for AML patients with AML1-ETO. Here, we report that AML1-ETO protein is rapidly degraded by Honokiol (HNK), a natural phenolic compound isolated from the plant *Magnolia officinalis*. HNK induced the degradation of AML1-ETO in a concentration- and time-dependent manner in leukemic cell lines and primary AML blasts with t(8;21) translocation. Mechanistically, HNK obviously increased the expression of UbcH8, an E2-conjugase for the degradation of AML1-ETO, through triggering accumulation of acetylated histones in the promoter region of *UbcH8*. Knockdown of *UbcH8* by small hairpin RNAs (shRNAs) prevented HNK-induced degradation of AML1-ETO, suggesting that UbcH8 plays a critical role in the degradation of AML1-ETO. HNK inhibited cell proliferation and induced apoptotic death without activation of caspase-3, which was reported to cleave and degrade AML1-ETO protein. Thus, HNK-induced degradation of AML1-ETO is independent of activation of caspase-3. Finally, HNK reduced the angiogenesis and migration in Kasumi-1-injected zebrafish, decreased xenograft tumor size in a xenograft leukemia mouse model, and prolonged the survival time in mouse C1498 AML model. Collectively, HNK might be a potential treatment for t(8;21) leukemia by targeting AML1-ETO oncoprotein.

© 2016 Elsevier Inc. All rights reserved.

1. Introduction

Acute myeloid leukemia (AML) is characterized by the blockage of differentiation or maturation of myeloid progenitor cells at different stages [1]. Acquired genetic changes, especially specific reciprocal chromosome translocations, greatly facilitate leukemogenesis. The t(8;21)(q22;q22) translocation, which juxtaposes the *AML1* gene on chromosome 21 with the *ETO* (eight-twenty-one) gene on chromosome 8, produces the *AML1-ETO* fusion gene. AML1-ETO translocation is one of the most frequently occurred chromosomal abnormalities in AML. The resultant AML1-ETO protein is composed of the NH2-terminal portion of wild-type AML1

protein and the nearly entire protein sequence of ETO. Mechanistically, AML1-ETO plays a critical and initiating role in leukemic transformation through inhibiting normal AML1 function in a dominant-negative manner [2]. Although ectopic expression of AML1-ETO in hematopoietic cells inhibits differentiation and enhances the self-renewal capacity of hematopoietic stem cells, AML1-ETO itself is not sufficient to induce leukemogenesis. AML1-ETO rapidly induces leukemia in cooperation with other gene mutations, such as *Wilms' tumor-1* [3], *c-kit* [4], or *HIF-1 α* [5].

AML1-ETO exerts the dominant negative effect on AML1-dependent transcriptional activation through interacting with nuclear corepressors N-CoR and Sin3A to recruit the histone deacetylases to AML1-responsive promoters. This interaction finally results in a lower level of histone acetylation and less-accessible chromatin, leading to transcriptional silencing of genes such as *cathepsin G* [6] and *p14^{ARF}* [7]. Ectopic expression of AML1-ETO enhances cell proliferation and inhibits cell differentiation towards granulocytic, monocytic or erythroid cells [8]. In

* Corresponding author at: Laboratory of Internal Medicine, The First Affiliated Hospital of Wenzhou Medical University, Shangcai Village, Nanbaixiang, Ouhai District, Wenzhou 325000, Zhejiang Province, China.

E-mail address: 782917063@qq.com (S. Gao).

¹ These two authors contributed equally to this work.

agreement with this, knockdown of AML1-ETO by small interfering RNA restores myeloid differentiation and inhibits leukemic clonogenicity [9]. Similarly, degradation of AML1-ETO by compounds such as oridonin [10] and histone deacetylase inhibitor [11] showed special anti-leukemia activity for the AML patients with AML1-ETO. Therefore, these data indicate that targeting AML1-ETO might contribute to the clinical effects of t (8;21) AML.

Honokiol (HNK), a natural phenolic compound isolated from the stem and bark of the plant *Magnolia officinalis* [12], exerts potential anti-neoplastic and anti-angiogenic activities through targeting multiple signaling including Wnt1- β -catenin [13], JAK2/STAT3 [14,15], and epidermal growth factor receptor (EGFR) [16]. For example, low concentration of HNK induced paraptosis but high concentration of HNK induced apoptosis in NB4 and K562 cells [17]. Meanwhile, our previous data showed that HNK inhibited constitutive and inducible STAT3 signaling via increasing SHP1 expression in AML cells [15] and HNK presented anti-leukemia activity through inhibiting histone deacetylases [18]. Although several compounds demonstrate strong anti-leukemia activity through degrading AML1-ETO protein [10,19], the preclinical or clinical effects are still poor. Thus, finding small-molecule inhibitors which both effectively degrade AML1-ETO protein and present anti-leukemia activity *in vitro* and *in vivo* might contribute to the clinical treatment for AML patients with AML1-ETO. However, it remains unclear whether HNK can degrade AML1-ETO protein through modulating ubiquitin-proteasome pathway.

In this report, we discover that HNK degrades AML1-ETO protein in leukemic cell lines and primary AML blasts. HNK increases the expression of E2-conjugase UbcH8 for the degradation of AML1-ETO, through triggering accumulation of acetylated histones in the promoter region of *UbcH8*. Additionally, HNK decreased xenograft tumor size and prolonged the survival time in mouse AML model through degradation of AML1-ETO protein. As a natural compound, without obvious side effects, HNK may be a potential anti-leukemia agent that targets AML1-ETO oncoprotein.

2. Materials and methods

2.1. Cell lines, primary AML blasts, and reagents

Human leukemic cell lines and murine AML cell line C1498 (ATCC, Manassas, VA, USA) were purchased for the present study. U937-AML1-ETO stable transformant (U937-A/E9/14/18, U937T) was generated as described [20,21]. U937T cells were treated with 5 μ M ponasterone A (Pon A, Santa Cruz Biotechnology, Santa Cruz, CA, USA) to induce AML1-ETO expression [21]. Bone marrow mononuclear cells (blasts% >70%) isolated by Ficoll density gradient centrifugation (GE Healthcare, Uppsala, Sweden) were obtained from 2 AML patients with positive AML1-ETO. All procedures performed in studies involving human participants were in accordance with the ethical standards of the Ethics Committee of the First Affiliated Hospital of Wenzhou Medical University and the Declaration of Helsinki. These patients all gave informed consent in accordance with the Declaration of Helsinki. Purified HNK (Sigma-Aldrich, St Louis, MO, USA), Proteasome inhibitor MG132 (Calbiochem, Gibbstown, NJ, USA), pancaspase inhibitor Z-VAD-FMK (Beyotime Institute of Biotechnology, Jiangsu Province, China), trichostatin A (TSA, Beyotime Institute of Biotechnology), 3-Methyladenine (3-MA, Sigma-Aldrich), and Cycloheximide (CHX, Sigma-Aldrich) were dissolved in dimethyl sulfoxide (DMSO). NSC606985 (kindly provided by Prof. Yingli Wu, Department of Pathophysiology, Shanghai Jiao Tong University School of Medicine) was dissolved in double distilled water. All these compounds were kept at -20°C until use.

2.2. mRNA extract and quantitative real-time PCR (qRT-PCR)

Total RNA was extracted by TRIzol (Invitrogen, Carlsbad, CA, USA) according to the manufacturer's instruction. RNA concentration and quality were analyzed by detecting the absorbance at 260 nm with Beckman DU6400 spectrophotometer (Beckman Counter, Miami, FL, USA). Relative expression was calculated using the $2^{-\Delta\Delta\text{CT}}$ method. The primers of AML1-ETO were according to previous reports [22,23] and primers of other gene transcripts were shown in Table 1.

2.3. Chromatin immunoprecipitation assay

The acetylation levels of gene promoter associated with ac-H3 and ac-H4 were examined by using Chromatin Immunoprecipitation (ChIP) Assay Kit (Merck-Millipore, Billerica, MA, USA) according to the manufacturer's instruction. Briefly, treated and untreated leukemic cells were cross-linked with 1% formaldehyde for 10 min. Nuclear extracts were extracted and chromatin was sonicated to generate 200–1000 bp DNA fragments. Protein-DNA complexes were immunoprecipitated with 5 μ g of specific antibodies (anti-acetylated histone H3, anti-acetylated histone H4 and non-relevant rabbit immunoglobulin G). DNA was purified from the protein-DNA cross-link, which was reversed by heating at 65°C for 4 h. Standard PCR reactions were performed with primer pairs (Table 1). PCR products were subjected to electrophoresis. Also, the immunoprecipitated DNA was analyzed by qRT-PCR and the amount of precipitated DNA was calculated as the percentage of the input sample.

2.4. Apoptosis detection

Leukemic cells were plated at 2×10^5 cells/ml in six-well plate. Apoptosis was detected by annexin V (Invitrogen) in combination with propidium iodide (Invitrogen). Cells treated with HNK were collected and washed with binding buffer, then incubated in working solution (200 μ l binding buffer with 0.5 μ l Annexin V-FITC and 0.1 μ l PI) for 15 min in dark. Cells were washed and resuspended with binding buffer. Samples were analyzed by flow cytometry (Becton Dickinson, Mountain View, CA, USA) within 30 min after staining.

2.5. Construction of plasmids

To produce UbcH8 (UBE2L6; NM_004223) overexpression plasmid, human UbcH8 coding sequence was amplified by PCR and then cloned into retrovirus vector pMSCV-puro (Clontech, Palo Alto, CA, USA) pCMV (Clontech). Gene-specific short hairpin RNAs (shRNAs) for UbcH8 were designed and cloned into retroviral vector pSIREN-RetroQ (Clontech). MSCV-puro-AML1-ETO (MSCV-A/E) was kindly provided by Prof. Ying Lu (Department of Pathophysiology, Shanghai Jiao Tong University School of Medicine). All the primer sequences for plasmid construction are shown in Table 1.

2.6. Retrovirus production and cell transfection

HEK293T cells (4×10^6) were plated in 10 cm dish. After 24 h, MSCV-puro-UbcH8, MSCV-puro-AML1-ETO, pSIREN-UbcH8, or negative control vectors were co-transfected with packaging plasmids Gap-pol and VSV-G vectors into HEK293T cells. Virus was harvested from the supernatant at 48 h posttransfection, and further filtered through a 0.45 μ m low protein-binding-polysulfonic filter (Merck-Millipore). Leukemic cells (2×10^5 /ml) were suspended in viral supernatant with 8 μ g/ml polybrene (Sigma-Aldrich, St. Louis, MO, USA) and centrifuged at 2000 rpm for 2 h.

Table 1

The sequences of primers for qRT-PCR, ChIP, and construction of plasmids.

Primer	Sequence (5'-3')
BCL-2-L	ATC CAG GAT AAC GGA GGC TG
BCL-2-R	GAA ATC AAA CAG AGG CCG CA
G-CSFR-L	ACC TCT CCT GCC TCA TGA AC
G-CSFR-R	CAG AGT GAA GCT GGT GGG TA
MPO-L	TGA TCG GTT TTG GTG GGA GA
MPO-R	ATG ATC CGG GGC AAT GAG AT
GM-CSF-L	ACT TCC TGT GCA ACC CAG AT
GM-CSF-R	CCA GCA GTC AAA GGG GAT GA
UbcH8-L	AGA CCG AAT ATC AGG GAG CC
UbcH8-R	TGA ACA GCT CCG GAT TCT GT
GAPDH-L	GGT CCG AGT CAA CGG ATT TG
GAPDH-R	ATT AGC CCC AGC CTT CTC CAT
SIAH1-L	TGA CTG GGT GAT GAT GCA GT
SIAH1-R	ATT GCG AAG AAC TGC TGG TG
sh-UbcH8#1	GCT GGT GAA TAG ACC GAA TAT
sh-UbcH8#2	GGA CGA GAA CGG ACA GAT T
sh-NC	GTT CTC CGA ACG TGT CAC GT
MSC	CCG CTC GAG ATG ATG GCG AGC
V-UbcH8-L	ATG CGA GT
MSC	CGG AAT TCT TAG GAG GGC CGG
V-UbcH8-R	TCC ACT C
CMV-UbcH8-L	CGG GAT CCA TGA TGG CGA GCA TGC GAG T
CMV-UbcH8-R	GGA ATT CTT AGG AGG GCC GGT CCA CT C
UbcH8C1-L*	CAG GGC GAG TGT GTA TTT GG
UbcH8C1-R*	GCT CAT ACG GGT TCC AGT CT
UbcH8C2-L*	AGA CTG GAA CCC GTA TGA GC
UbcH8C2-R*	GCC TCC CCG CAC CCG CTC CG

* Sequences for ChIP analysis.

Puromycin (2 µg/ml, Medchemexpress, Princeton, NJ, USA) was added into the supernatant for one week to select positive clones.

2.7. HDAC enzyme activity

Relative HDAC enzyme activity was measured by the colorimetric HDAC Activity Assay Kit (566328, Merck-Millipore) following the manufacturer's instruction. Briefly, samples were incubated with the HDAC assay substrate, allowing deacetylation of the substrate. Cells were incubated with HNK and then lysed with RIPA lysis buffer supplemented with protease inhibitors. The protein extracts were incubated with assay buffer containing HDAC assay substrate for 60 min at 37 °C. Then, the activator solution released *p*-nitroanilide from the deacetylated substrate or standard. The absorbance was read at 405 nm. The relative HDAC enzyme activity was calculated by standard curve. The untreated samples were arbitrarily set as 1.0.

2.8. Western blot

Western blot analysis was performed using standard techniques. The following antibodies were used: AML1 (#4334S, Cell Signaling Technology, Beverly, MA), ETO (sc-9737, Santa Cruz Biotechnology, Santa Cruz, CA, USA), SIAH-1 (sc-5505, Santa Cruz Biotechnology), UbcH8 (ab109086, Abcam, Cambridge, MA, USA), caspase-3 (ab32351, Abcam), ac-H3 (382158, Merck-Millipore), ac-H4 (382160, Merck-Millipore). As necessary, blots were stripped and reprobed with β-actin antibody (04-1116, Merck-Millipore) as an internal control. Signals were measured by chemiluminescence reagents (Merck-Millipore). All experiments were repeated three times with the similar results. Signal intensity of proteins was normalized against β-actin using Quantity One (Bio-Rad, Richmond, CA, USA) and statistically analyzed. The fold change compared with untreated control was arbitrarily assigned a unit of 1.0 in each case.

2.9. Embryo collection and microinjection of zebrafish experiments

Wild-type zebrafishes (*Danio rerio*) were maintained, and embryos were collected and staged. Embryos were kept in E3 medium at 28.5 °C with 0.003% 1-phenyl-2-thiourea (PTU, Sigma-Aldrich) to inhibit pigmentation. Before injecting into zebrafish larvae, all cells were labeled with CM-Dil, a lipophilic fluorescent tracking dye (Invitrogen), at 48 h post fertilization (hpf.). At least 100 embryos should be used in each experimental and control groups. The final concentration of HNK was 4 µM in E3 medium. Staining was performed by the BCIP/NBT Alkaline Phosphatase Color Development Kit (Beyotime Institute of Biotechnology, Jiangsu, China) according to the manufacturer's instruction. The images were captured by Stereomicroscope (Olympus, Tokyo, Japan).

2.10. Microarray analysis

The total RNA was extracted from Kasumi-1 cells treated with 40 µM HNK or not for 24 h. Then, the total RNA was converted to cDNA by SuperScript II reverse transcriptase (Invitrogen) and was amplified. The cDNA was then hybridized onto the Human gene-Chip® 3'IVT Express Kit (Affymetrix, Santa Clara, CA, USA). Quantile normalization and subsequent data processing were performed using Partek GS 6.5 software package (Affymetrix). All genes represented by the array showed a single peak on the melting curve characteristic to the specific products. Excel-based PCR Array Data Analysis Software provided by manufacturer was used for analysis of gene expression. The microarray analysis was completed in Gene Tech (Shanghai) Company Limited (Gene Tech, Shanghai, China).

2.11. Co-immunoprecipitation

4 × 10⁶ 293T-MSCV-AML1-ETO cells transfected with pCMV-NC or pCMV-UbcH8 were harvested with immunoprecipitation lysis buffer (150 mM NaCl; 20 mM Tris-HCl, pH 7.6; 1 mM EDTA; 0.5% NP-40; 1 mM PMSF; 10% glycerol; protease inhibitor cocktail). After brief sonication, the lysates were centrifuged (17,000g, 15 min) at 4 °C. After pre-clearing with normal IgG at 4 °C for 2 h, supernatants were incubated with antibody against Ubiquitin (Abcom; ab7780) or normal mouse IgG (Santa Cruz, sc2343) together with protein A plus-agarose (Santa Cruz, sc2003) overnight at 4 °C. After immunoprecipitation the beads were washed five times with washing buffer (300 mM NaCl; 1 mM EDTA; 50 mM Tris-HCl; 0.5% NP-40; 10% glycerol), then precipitates were analyzed by western blot.

2.12. Murine model of *t*(8;21) leukemia

Male athymic nude mice and C57 mice (4-week-old) were purchased from SLAC (Shanghai SLAC Laboratory Animal, Shanghai, China) and were housed in blanket cages facilities with a 12 h light dark cycle, with food and water available. All animal procedures and care were conducted in accordance with institutional guidelines of Wenzhou Medical University and in compliance with national and international laws and policies. For xenograft model in nude mice, 1 × 10⁷ viable Kasumi-1 cells mixed with high concentration of Matrigel™ Matrix (1:1 ratio, BD Bioscience, San Jose, CA, USA) were injected subcutaneously into right flank of each nude mouse. After 2 weeks, mice were randomly divided into two groups. One group of mice (n = 5) was treated with intraperitoneal injections of HNK (3 mg/mouse/day) [24] dissolved in 20% Intralipid (Sigma-Aldrich), three times per week. The other group of mice (n = 5) received an equal volume of Intralipid and served as a control group. Mice were sacrificed and the tumors from each

mouse were harvested when the experiment was terminated at 6 weeks after tumor cell inoculation. The volumes of tumors and wet weights were recorded. Tumor volumes were measured using the equation $V (\text{in mm}^3) = A \times B^2/2$, where A is the largest diameter and B is the perpendicular diameter. The tumor tissues from all groups were rapidly frozen in liquid nitrogen for later use.

Murine leukemic cell line C1498 was transfected with lentivirus vector pLVX-IRES-ZsGreen1 (Clontech), followed with selection by flow cytometry and named C1498-GFP. C1498-GFP cells were transfected with MSCV-A/E or MSCV-NC, followed with puromycin selection for one week. C1498-GFP cells carrying AML1-ETO was called C1498-GFP-A/E. Male C57 mice received 400 cGy from a high-energy linear accelerator (Siemens Primus, Siemens, New York, NY). After 24 h, C57 mice (n = 12) were intravenously injected with 5×10^6 C1498-GFP-A/E. Six days after leukemic cell transplantation, the C57 mice received intraperitoneal injections with vehicle (n = 6) or intraperitoneal injections of HNK (3 mg/mouse/day) dissolved in 20% intralipid (Sigma-Aldrich) per day (n = 6) [24]. Bone marrow mononuclear cells were extracted for Wright's staining and further for western blot. When the mice became moribund, they were humanely killed and survival was evaluated from the first day of experiment until death.

2.13. Statistical analysis

All the results were expressed as Mean \pm SD where applicable. The significance of the difference between groups was determined by Student's *t*-test. A *P* value of less than 0.05 was considered statistically significant. All statistical analyses were performed with SPSS software (SPSS 22.0, Chicago, IL, USA).

3. Results

3.1. HNK induces the degradation of AML1-ETO protein

To determine whether AML1-ETO protein is degraded by HNK (Fig. 1A), Kasumi-1 cells carrying endogenous AML1-ETO were treated with 10, 20, and 40 μM HNK for different times, because our previous results indicated that 40 μM HNK effectively inhibited cell proliferation in leukemic cells [15,18]. HNK degraded AML1-ETO fusion protein in a time- and concentration-dependent manner through anti-AML1 and anti-ETO antibody, respectively (Fig. 1B–D). Because the N-terminal DNA binding domain of the AML1 is fused to nearly all of the ETO, we then address whether wide-type AML1 protein is altered by HNK. Also, HNK degraded wide-type AML1 protein in a time- and concentration-dependent manner in Kasumi-1 cells (Fig. 1B–D). However, HNK failed to change AML1-ETO mRNA expression in Kasumi-1 cells (Fig. 1E). To address whether HNK can degrade exogenous AML1-ETO protein, U937T cells, which conditionally express the AML1-ETO protein when it is treated by Pon A [21], were treated for HNK. Pon A effectively induced AML1-ETO expression (Fig. 1F). Accordingly, HNK degraded AML1-ETO protein in a concentration- and time-dependent manner in Pon A-induced U937T cells (Fig. 1G–I). To further confirm that HNK degrades AML1-ETO protein in primary leukemic samples, bone marrow mononuclear cells from 2 AML patients with t(8;21) translocation were treated with 40 μM HNK for 48 h. Similarly, HNK degraded AML1-ETO protein (Fig. 1J). Finally, to determine whether HNK can also degrade AML1-ETO protein in non-leukemic cell line, 293T cells were transfected with MSCV-A/E to constitutively express AML-ETO protein (Fig. 1K) and treated with HNK for 24 h. As expected, HNK degraded AML1-ETO protein in 293T-MSCV-A/E cells (Fig. 1L).

Furthermore, we determine whether AML1-ETO-targeted genes are regulated by HNK. As reported [10], AML1-ETO induces the expression of apoptotic antagonist BCL-2, granulocyte colony-stimulating factor receptor (G-CSFR) as well as myeloperoxidase (MPO) and blocks transactivation of the granulocyte-macrophage colony-stimulating factor (GM-CSF). Accordingly, HNK decreased the mRNA expressions of BCL-2, G-CSFR, and MPO (Fig. 1M and N), and at the same time increased the expression of GM-CSF in Kasumi-1 cells and U937T cells (Fig. 1O and P).

3.2. Analyze target genes by microarray analysis

To analyze possible target genes by HNK, microarray analysis was used to compare mRNA expression before and after HNK treatment. Almost 1168 different genes were increased (>2-fold) and 212 different genes (<-2-fold) were decreased by HNK (Fig. 2A and B). UbcH8, an E2-conjugase [25], which was increased about 4-fold by HNK, was further evaluated, because UbcH8 is mediated in the degradation of AML1-ETO [26] (Fig. 2C). Finally, although signaling pathway analysis did not directly indicate that ubiquitin-proteasome pathway was modulated by HNK, pathways concerning degradation of protein such as autophagic vacuole and phagocytic vesicle were increased by HNK (Fig. 2D).

3.3. The role of UbcH8 in HNK-induced degradation of AML1-ETO

The observation that HNK decreased the protein but not mRNA expression of AML1-ETO prompted us to determine whether HNK degraded AML1-ETO protein at the post-transcriptional level. For this purpose, Kasumi-1 cells were treated with 10 $\mu\text{g/ml}$ protein synthesis inhibitor cycloheximide (CHX) with or without HNK for different times. The half-life of AML1-ETO protein was obviously shorter in HNK-treated Kasumi-1 cells compared with untreated cells (Fig. 3A), indicating that the stability of AML1-ETO was lower upon HNK treatment. To determine whether HNK degrades AML1-ETO through the ubiquitin-proteasome system [26], Kasumi-1 and U937T cells were treated with HNK in the presence with MG132, a prototypical proteasome inhibitor [27]. MG132 almost prevented HNK-induced degradation of AML1-ETO protein (Fig. 3B).

To confirm the microarray results that UbcH8 was increased by HNK, Kasumi-1 and U937T cells were treated with 40 μM HNK for 24 and 48 h. HNK significantly increased the mRNA expressions of UbcH8 in both cell lines (Fig. 3C). Also, HNK increased the protein levels of UbcH8 in Kasumi-1 cells for 24 and 48 h. By contrast, HNK only increased the protein levels of UbcH8 in U937T cells for 48 h but not for 24 h (Fig. 3D). In addition, HNK increased the protein expression of UbcH8 in 2 primary AML blasts carrying AML1-ETO (Fig. 3E). Furthermore, HNK increased the protein level of UbcH8 in another two leukemic cell lines THP1 and HEL without AML1-ETO (Fig. 3F). To determine whether the increased expression of UbcH8 contributes to the degradation of AML1-ETO, Kasumi-1 and U937T cells were transfected with retrovirus MSCV-UbcH8 or negative control. Overexpression of UbcH8 in both cell lines effectively induced degradation of AML1-ETO (Fig. 3G). To further determine whether UbcH8 enhances the accumulation of ubiquitination of AML1-ETO, 293T-MSCV-AML1-ETO cells were transiently transfected with negative control or pCMV-UbcH8, followed by the co-immunoprecipitation (co-IP) with anti-ubiquitin antibody or anti-AML antibody. As indicated in Fig. 3H and I, overexpression of UbcH8 significantly increased the accumulation of ubiquitination of AML1-ETO.

To address whether UbcH8 plays an important role in HNK-induced degradation of AML1-ETO protein, UbcH8 was knocked down by specific shRNA. UbcH8 protein expression was effectively reduced by two independent shRNAs in Kasumi-1 and U937T cells (Fig. 3J). Furthermore, Kasumi-1 and U937T cells, in which UbcH8

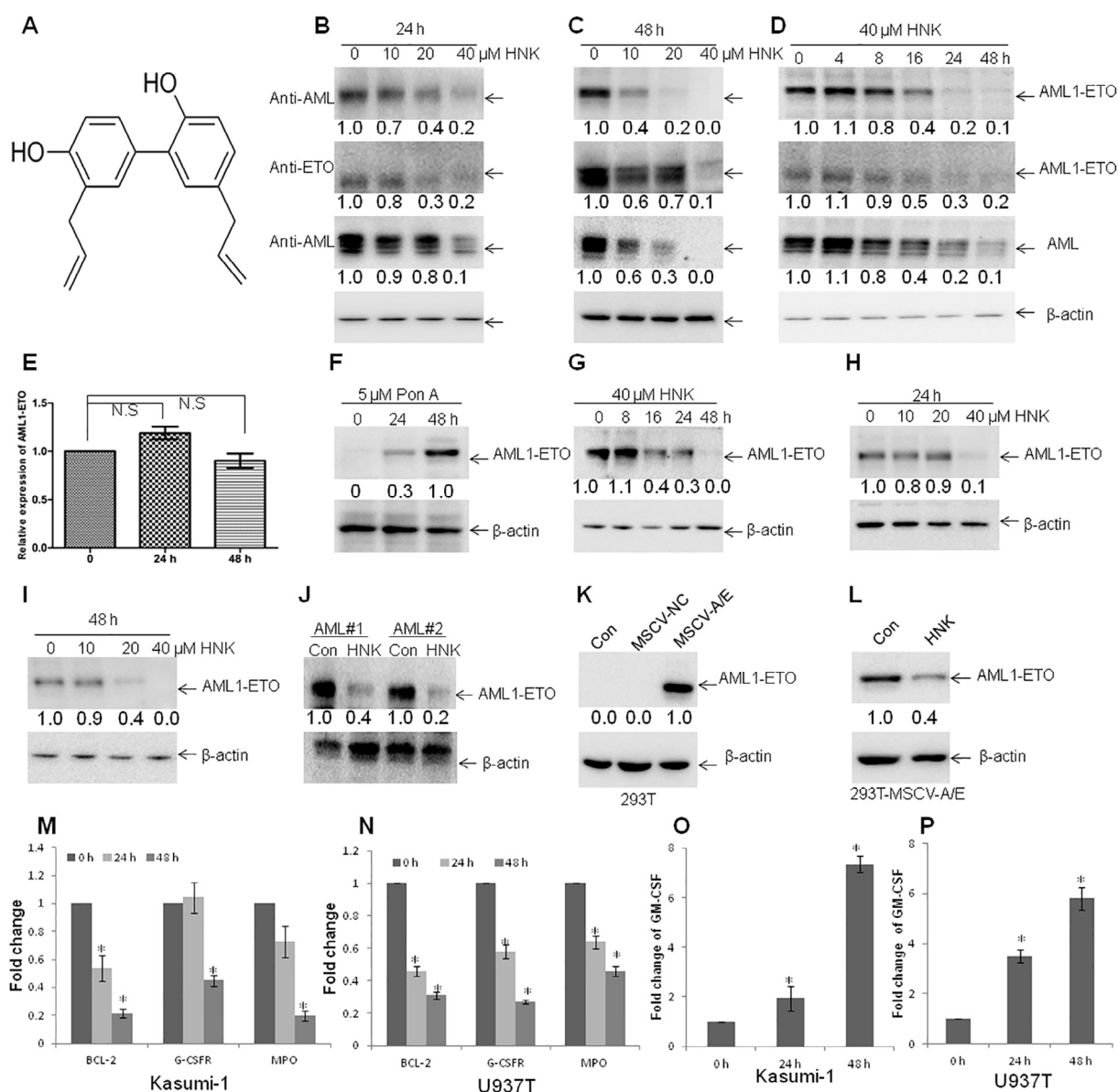


Fig. 1. HNK induces degradation of AML1-ETO protein. (A) The chemical structure of HNK. (B–D) The expression of AML1-ETO fusion protein was measured by western blot through anti-AML1 or anti-ETO antibody in Kasumi-1 cells treated with different concentrations of HNK for 24 (B) and 48 h (C) and 40 μ M HNK for different times (D). Alternatively, AML1 protein was detected through anti-AML1 antibody. (E) The mRNA expression of AML1-ETO was detected by qRT-PCR in Kasumi-1 cells treated with 40 μ M HNK for 24 and 48 h. Values are expressed as mean \pm SD (n = 3). (F) The protein level of AML1-ETO was detected in U937T cells treated with 5 μ M Pon A for 24 and 48 h. (G) The expression of AML1-ETO was detected in Pon A-treated U937T cells, which were incubated with 40 μ M HNK for the indicated times. (H and I) The protein level of AML1-ETO was detected in Pon A-treated U937T cells treated with 10, 20, and 40 μ M HNK for 24 and 48 h. (J) Bone marrow mononuclear cells (blasts >70%) were isolated from 2 AML patients with positive AML1-ETO. The protein expression of AML1-ETO was measured in these cells treated with 40 μ M HNK for 48 h. (K) 293T cells were transfected with MSCV-A/E or negative control, followed with selection of puromycin (2 μ g/ml) for one week and detection of AML1-ETO expression by western blot. (L) 293T cells expressing AML1-ETO were treated with 40 μ M HNK for 24 h, and then AML1-ETO expression was measured. The relative intensity of each band after normalization for β -actin is shown under each blot as the fold change compared with untreated control, which was arbitrarily assigned a unit of 1.0 in each case. All experiments were repeated three times. (M–P) The mRNA expressions of BCL-2, G-CSFR, MPO, and GM-CSF were detected by qRT-PCR in Kasumi-1 (M and O) and U937T cells (N and P) treated with 40 μ M HNK for 24 and 48 h. * P < 0.01 versus untreated cells. Values are expressed as mean \pm SD (n = 3).

was stably knocked down, were treated with HNK. The degradation of AML1-ETO by HNK was almost prevented by knockdown of UbcH8 (Fig. 3K and L).

Because E3-ligase SIAH-1 also plays an important role in the degradation of AML1-ETO [26], we further assess whether HNK modulates the expression of SIAH-1. Kasumi-1 and U937T cells were treated with 40 μ M HNK for 24 and 48 h, the mRNA and protein expressions of SIAH-1 were measured. Interestingly, HNK only slightly increased the expression of SIAH-1 in Kasumi-1 and U937T cells (Fig. 3M and N).

3.4. The anti-leukemia activity of HNK in Kasumi-1 and U937T cells

Previous data showed that AML1-ETO protein was cleaved into four fragments by active caspase-3 in apoptotic condition [20]. HNK induced apoptosis with the activation of caspase-3 in B-cell chronic lymphocytic leukemia [28]. However, HNK induced paraptosis in NB4 and K562 cells, a novel form of non-apoptotic programmed cell death without activation of caspase-3 [29]. These inconsistent results prompted us to investigate whether HNK induces the degradation of AML1-ETO through caspase-3-independent cleavage. Although 40 μ M HNK led to 15% of apopto-

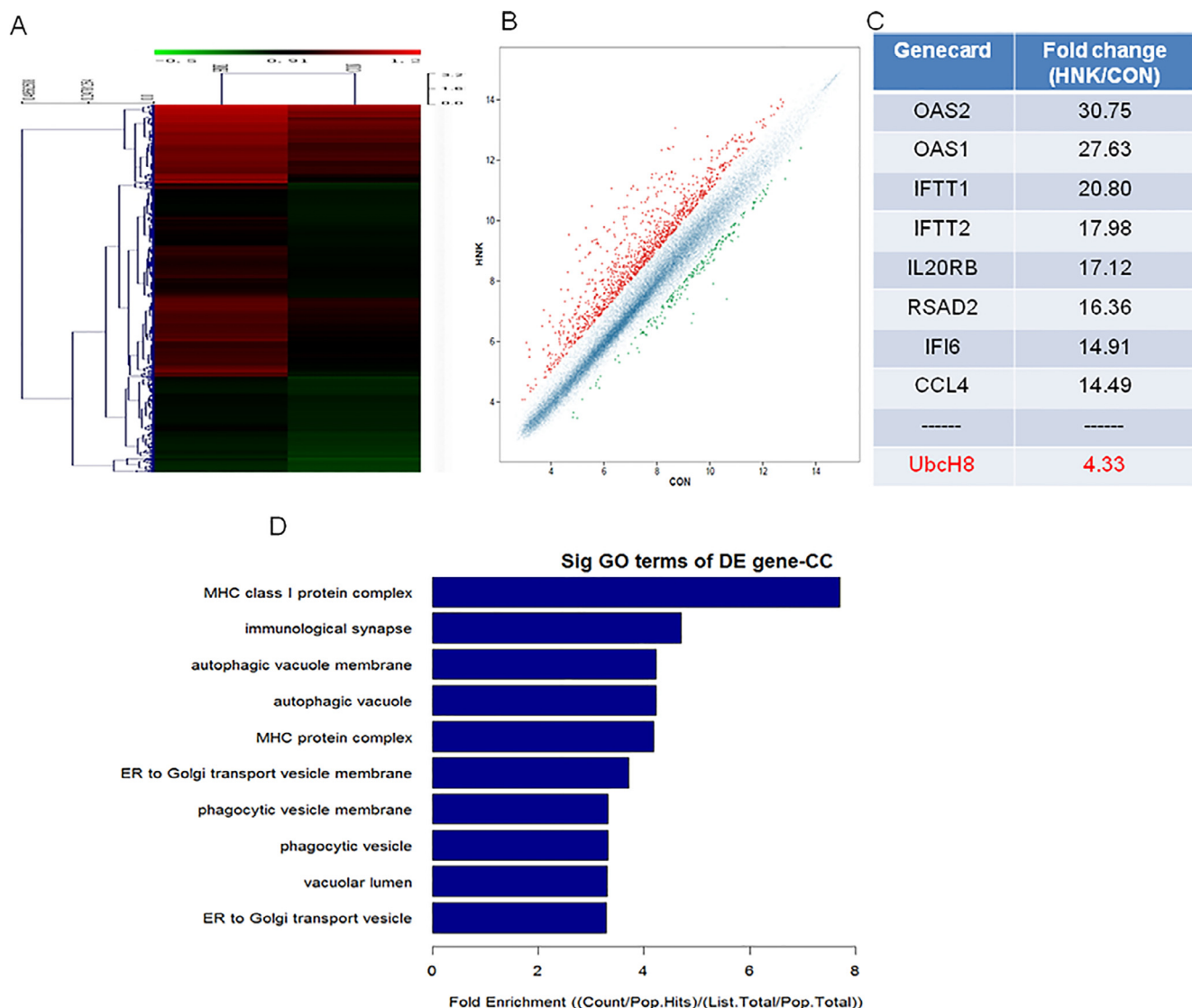


Fig. 2. Microarray analysis for selecting HNK-regulated genes. (A) Heatmap representation of genes. (B) Scatter plots were indicated for the genes, which are upregulated (red plot) and downregulated (green plot) above 2-fold by HNK. (C) Ranked genes including Ubch8 were significantly increased by HNK. (D) Signaling pathways including phagocytic vesicle and autophagic vacuole were altered by HNK. (For interpretation of the references to color in this figure legend, the reader is referred to the web version of this article.)

sis in Kasumi-1 cells (Fig. 4A and B) and 40% of apoptosis in U937T cells (Fig. 4C and D), respectively, HNK failed to induce activation of caspase-3 (Fig. 4E and H) and PARP (Fig. 4F and I). NSC606985-treated leukemic cells were used as positive controls, because NSC606985 significantly triggered Kasumi-1 and U937T cells to undergo apoptosis with activation of caspase-3 and PARP [20]. To further rule out the possibility that apoptosis causes the destabilization of AML1-ETO protein, leukemic cells were pre-treated with the cell-permeable pan-caspase inhibitor Z-VAD-FMK, followed with HNK treatment. The degradation of AML1-ETO by HNK was not blocked by Z-VAD-FMK (Fig. 4G and J). Finally, HNK induced time- and concentration-dependent growth inhibition and cell death in both cell lines (Fig. 4K–N). To determine whether U937 cells were sensitive to HNK as well as U937T, viability was measured in U937 cells treated with different concentrations of HNK for 24 and 48 h. Our data showed that U937 cells have the same sensitivity to HNK compared with U937T cells (Fig. 4O).

To further explore whether knockdown of Ubch8 affects the anti-leukemia effect by HNK, Kasumi-1 and U937T cells were transfected with shRNAs for Ubch8, followed with treatment by

HNK. Knockdown of Ubch8 partially prevented HNK-induced cell death (Fig. 4P). Finally, we determine whether overexpression of Ubch8 affects cell viability. As indicated in Fig. 4Q, overexpression of Ubch8 reduced cell viability in Kasumi-1 and U937T cells.

Besides ubiquitin-proteasome system, protein can also be degraded by autophagy. To rule out whether autophagy mediates HNK-induced degradation of AML1-ETO protein, Kasumi-1 cells were cultured with autophagy inhibitor 3-MA and HNK for 48 h. 3-MA failed to restore the degradation of AML1-ETO by HNK (Fig. 4R). These results were consistent with the report that autophagy cannot degrade AML1-ETO protein [30].

3.5. HNK triggers accumulation of acetylated histones in the promoter of Ubch8

Recently, several reports have indicated that HNK presents anti-HDAC activity and increases the expression of acetylated histones [18,31]. We then determine whether HNK increases the expression of Ubch8 through accumulating acetylated histones in the promoter of Ubch8. We firstly detected the HDAC activity in

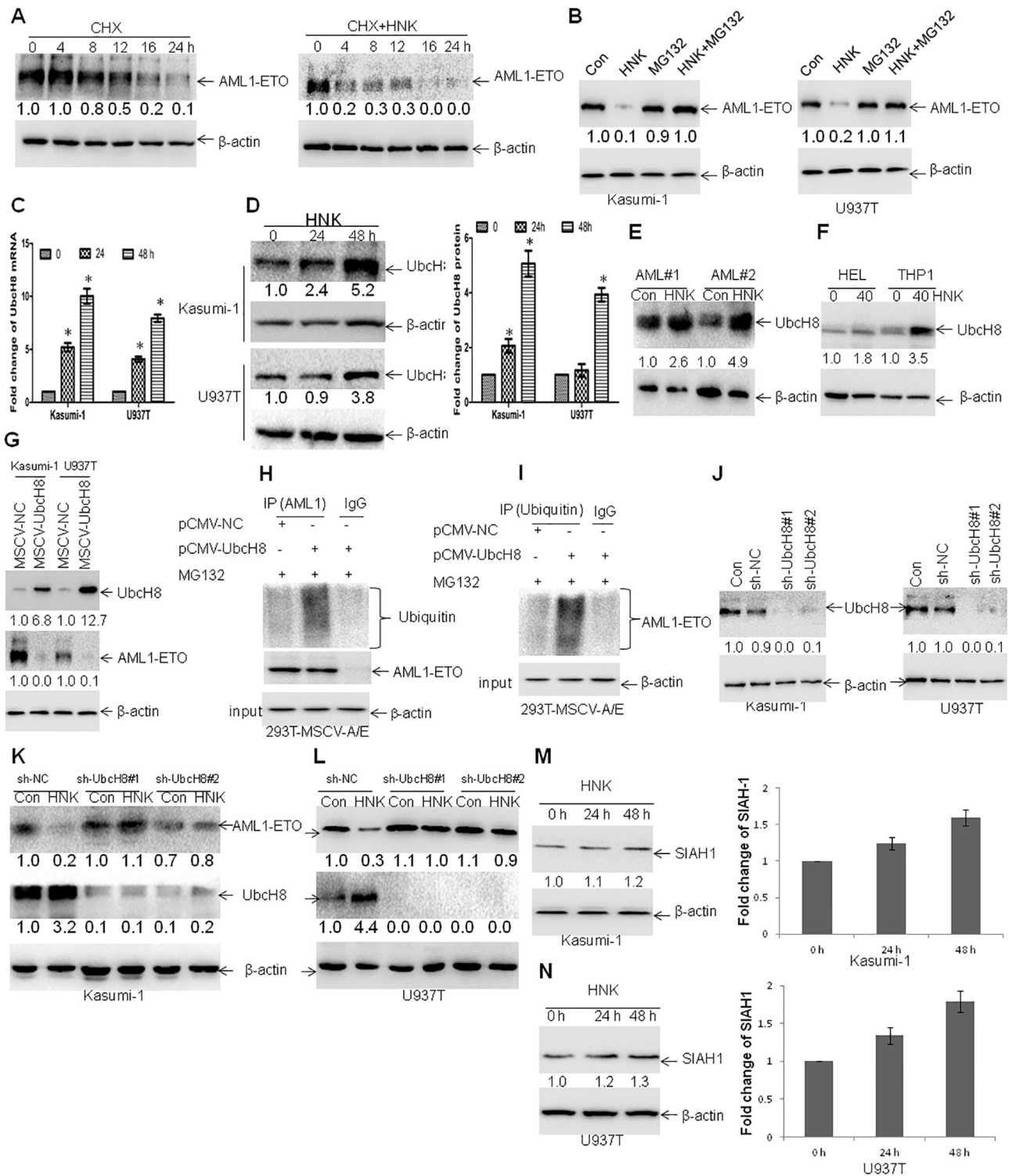


Fig. 3. The role of Ubch8 in HNK-induced degradation of AML1-ETO. (A) AML1-ETO expression was detected in 10 μ g/ml CHX-treated Kasumi-1 cells incubated with or without 40 μ M HNK for the indicated times. (B) The protein expression of AML1-ETO was measured in Kasumi-1 and U937T cells, which were treated with 40 μ M HNK for 48 h. The proteasome inhibitor MG-132 (5 μ M) was added 4 h before cell harvest. (C and D) Kasumi-1 and U937T cells were treated with 40 μ M HNK for 24 and 48 h, and then the mRNA (C) and protein (D) levels of Ubch8 were measured by qRT-PCR and western blot, respectively. Quantified results of Ubch8 protein were indicated in right of D. Values are expressed as mean \pm SD ($n = 3$). $^*P < 0.01$ compared with untreated cells. (E) Western blot was taken to detect Ubch8 protein level in bone marrow mononuclear cells from 2 AML patients with t(8;21) translocation, which were incubated with 40 μ M HNK for 48 h. (F) Leukemic cell lines HEL and THP1, which do not express AML1-ETO, were treated with 40 μ M HNK for 48 h. Ubch8 expression was detected. (G) The indicated proteins were detected in Kasumi-1 and U937T cells, which were transfected with retrovirus vectors MSCV-Ubch8 or MSCV-NC, followed with puromycin selection for one week. (H and I) 293T-MSCV-AML1-ETO cells were transiently transfected with negative control pCMV-NC or pCMV-Ubch8 for 48 h, followed by the co-immunoprecipitation (co-IP) with anti-AML antibody (H), anti-ubiquitin antibody (I), or normal mouse IgG. MG-132 (5 μ M) was added 4 h before cell harvest. The western blots were taken for the indicated proteins in co-IP complex and input by anti-ubiquitin antibody (H), anti-AML antibody (I), and anti- β -actin, respectively. (J) Kasumi-1 and U937T cells were transfected with two specific small hairpin RNAs (shRNAs) for Ubch8 or negative control (sh-NC), followed with puromycin selection for one week. Western blot was taken to detect Ubch8 expression. (K and L) The indicated proteins were detected in Kasumi-1 and U937T cells transfected with sh-Ubch8 or sh-NC and then treated with 40 μ M HNK or not for 48 h. (M and N) The protein and mRNA levels of SIAH1 were measured in Kasumi-1 (M) and U937T (N) cells treated with 40 μ M HNK for 24 and 48 h. The relative intensity of each band after normalization for β -actin is shown under each blot as the fold change compared with untreated control, which was arbitrarily assigned a unit of 1.0 in each case. All experiments were repeated three times.

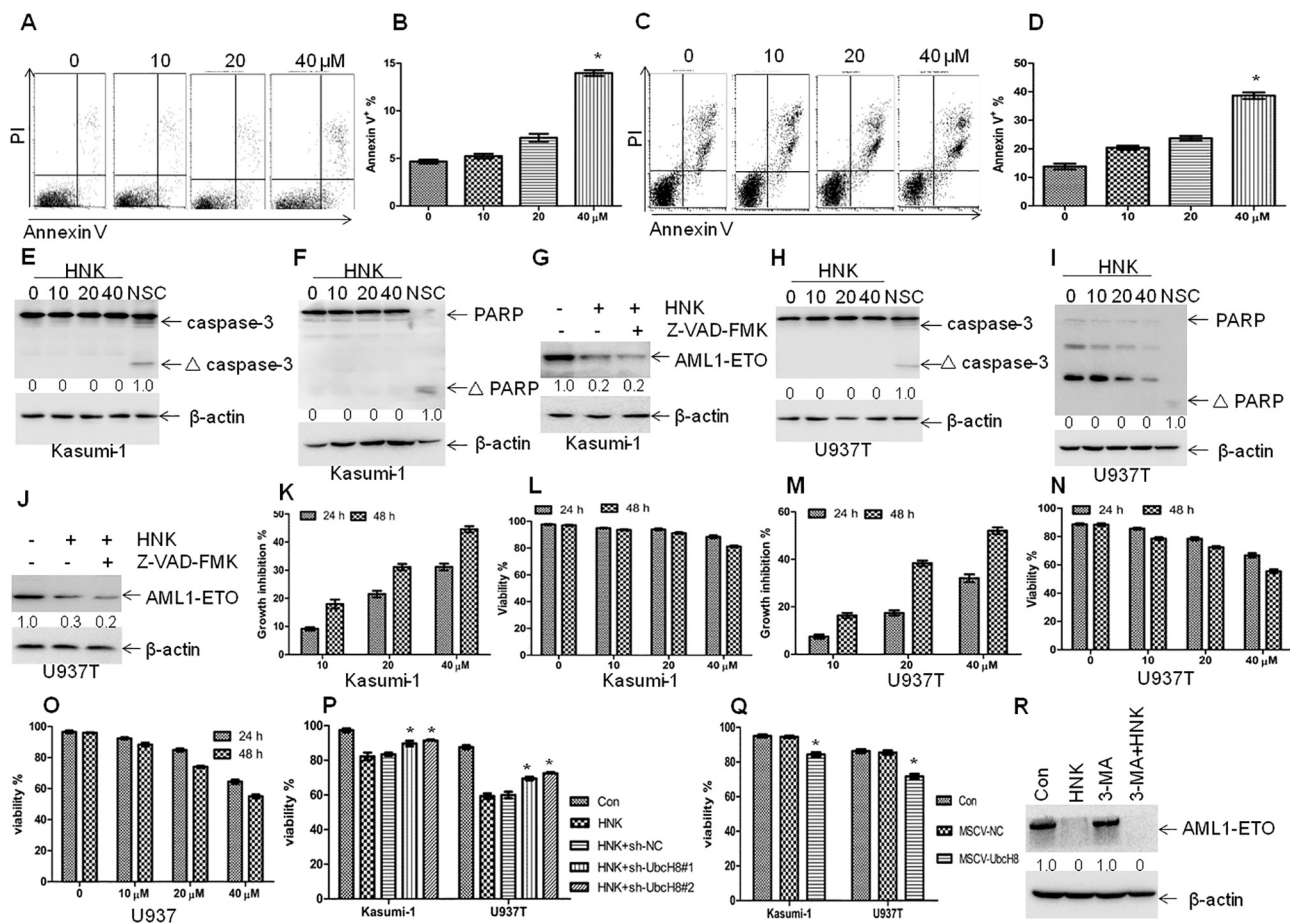


Fig. 4. HNK-induced apoptosis is independent of activation of caspase-3. (A–D) Apoptosis was determined by Annexin V/PI assay in Kasumi-1 cells (A and B) and U937T cells (C and D) treated with the indicated concentrations of HNK for 48 h. Values are expressed as mean \pm SD ($n = 3$). $^*P < 0.01$ compared with untreated cells. (E–J) Total caspase-3, active caspase-3, total PARP, and active PARP were detected in Kasumi-1 (E and F) and U937T cells (H and I) incubated with 10, 20, and 40 μM HNK for 48 h. NSC606985-treated cell lysates from Kasumi-1 and U937T were used for positive controls. AML1-ETO expression was detected in Kasumi-1 (G) and U937T cells (J) which were pre-treated with pan-caspase inhibitor Z-VAD-FMK (20 μM) for 1 h, followed with 40 μM HNK or not for 48 h. The relative intensity of each band after normalization for β -actin is shown under each blot as the fold change compared with untreated control. All experiments were repeated three times. (K–N) Growth inhibition rate was calculated according to viable cell numbers of treated cells against numbers of untreated cells in Kasumi-1 (K) and U937T cells (M), which were treated with indicated concentrations of HNK for 24 and 48 h. Viability was counted according to viable cell numbers against total cell numbers in Kasumi-1 (L) and U937T cells (N) treated with indicated concentrations of HNK for 24 and 48 h. (O) Viability was counted in U937 cells cultured with different concentrations of HNK for 24 and 48 h. (P) Viability was counted in Kasumi-1 and U937T cells transfected with sh-UbcH8#1, sh-UbcH8#2, or sh-NC and then treated with 40 μM HNK for 48 h. $^*P < 0.05$ compared with negative control. (Q) Viability was counted in Kasumi-1 and U937T cells, which were transfected with retrovirus vectors MSCV-UbcH8 or MSCV-NC for 48 h. $^*P < 0.05$ compared with negative control. (R) AML1-ETO protein was detected in Kasumi-1 cells, which were treated with autophagy inhibitor 3-MA (5 mM) and 40 μM HNK for 48 h.

Kasumi-1 and U937T cells treated with HNK. HDAC activity was obviously decreased by HNK in a concentration-dependent manner (Fig. 5A). Furthermore, acetylated histones (ac-H3 and ac-H4) were significantly increased in HNK-treated Kasumi-1 and U937T cells than untreated cells (Fig. 5B). Although HNK effectively reduced HDAC activity and increased the levels of ac-H3 and ac-H4 (Fig. 5A and B), it was not determined whether HNK modulated the levels of histone acetylation in *UbcH8* promoter region. To test it, Proscan (Version 1.7) was used to determine the possible promoter region of *UbcH8*. Promoter region predicted on forward strand was in -431 to -180 bp before the translation start and the Promoter Score was 59.26, which was above the Promoter Cutoff (53.00, Fig. 5C). Further, we designed two pairs of primer (Fig. 5D) surrounding the putative promoter region for ChIP to detect the levels of histone acetylation. As indicated in Fig. 5E and F, the band densities of UbcH8-associated acetylated histone proteins were obviously higher in chromatin that was extracted from HNK-treated cells than in chromatin extracted from untreated cells. Moreover, immunoprecipitated DNA from Kasumi-1 and U937T cells was analyzed by qRT-PCR. The levels of ac-H3

and ac-H4 in *UbcH8* promoter regions were increased about 2–6 folds in HNK-treated cells compared with untreated cells (Fig. 5G–J).

Previous data report that HDAC inhibitor VPA increases the expression of UbcH8 and degrades AML1-ETO protein [26]. To confirm it, Kasumi-1 cells were treated with another HDAC inhibitor TSA for 24 and 48 h. As indicated in Fig. 5K, TSA significantly decreased the expression AML1-ETO but increased the expression of UbcH8.

Given that AML1-ETO interacts with Heat shock protein 90 (HSP90) and HSP90 antagonist 17-allylamino-geldanamycin (17-AAG) induces the degradation of AML1-ETO [11], we then determine whether HNK induced-degradation of AML1-ETO is through degrading HSP90 protein. Kasumi-1 cells were treated with 40 μM HNK for 24 and 48 h. However, HNK failed to affect the protein expression of HSP90 in Kasumi-1 cells (Fig. 5L).

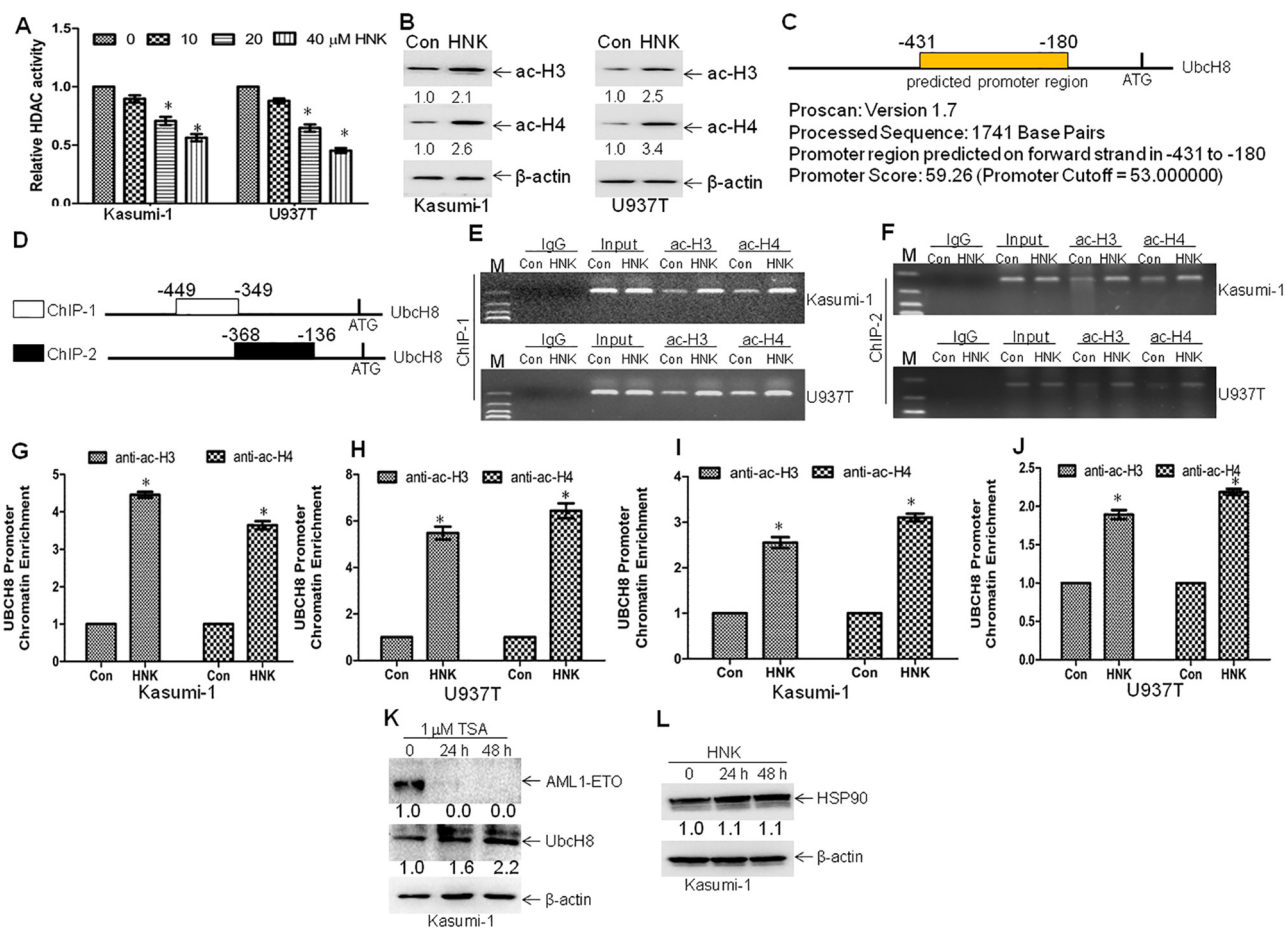


Fig. 5. HNK enhances accumulation of acetylated histones in the promoter of UbcH8. (A) HDAC activities were measured by colorimetric HDAC Activity Assay Kit in Kasumi-1 and U937T cells treated with indicated concentrations of HNK for 48 h. * $P < 0.01$ versus untreated cells. (B) The protein expressions of ac-H3 and ac-H4 were measured in Kasumi-1 and U937T cells treated with 40 μM HNK for 48 h. The relative intensity of each band after normalization for β -actin is shown under each blot as the fold change compared with untreated control. All experiments were repeated three times. (C) Proscan was used to predict putative promoter region of UbcH8. (D) A schematic representation of the promoter regions amplified by ChIP-PCR assay. (E and F) Soluble chromatin from Kasumi-1 and U937T cells treated with or without 40 μM HNK for 48 h was immunoprecipitated with anti-ac-H3 and anti-ac-H4 antibodies. Precipitated DNAs were analyzed by PCR with primer pairs of ChIP-1 and ChIP-2, followed with analysis by agarose gel electrophoresis. (G–J) Precipitated DNAs from Kasumi-1 and U937T cells were qualified by qRT-PCR with primer pairs of ChIP-1 (G and H) and ChIP-2 (I and J). The amounts of precipitated DNA were calculated as the percentage of the input sample. * $P < 0.01$ versus untreated cells. Values are expressed as mean \pm SD ($n = 3$). (K) AML1-ETO and UbcH8 expressions were detected in Kasumi-1 cells treated with 1 μM TSA for 24 and 48 h. (L) HSP90 expression was detected in Kasumi-1 cells treated with 40 μM HNK for 24 and 48 h. Representative western blots are shown. The relative intensity of each band after normalization for β -actin is shown under each blot as the fold change compared with untreated control, which was arbitrarily assigned a unit of 1.0 in each case. All experiments were at least repeated three times.

3.6. HNK decreases the angiogenesis and migration in Kasumi-1-injected zebrafishes

Recent studies have shown that zebrafish is a suitable model for the selection of compounds [32]. We incubated zebrafishes with different concentrations of HNK (2, 4, 8, 16, and 32 μM) for 72 h and found HNK ($\leq 4 \mu\text{M}$) did not cause zebrafish death. Thus, 4 μM HNK was used for the next tests. Kasumi-1 cells were labeled with CM-Dil and injected into 4.5–5.5 h zebrafish embryo yolk middle to evaluate vascular proliferation. HNK failed to affect the subintestinal vessels (SIV) and the neovessels, the latter originated from SIV basket (Fig. 6A), indicating that angiogenesis in normal zebrafish was not affected by HNK. However, the rate of neovessels in Kasumi-1-injected fishes is higher than that in non-injected fishes (Fig. 6C, Column 1 versus Column 3). HNK obviously decreased the rate of neovessels in Kasumi-1-injected zebrafishes (Fig. 6B and C Column 3 versus Column 4). Kasumi-1 cells were injected into 2-day old zebrafish larvae, which are permeable to small molecules, to analyze metastasis. Similarly, HNK obviously decreased the migration in Kasumi-1-injected fishes (Fig. 6D and E).

3.7. Effects of HNK in a Kasumi-1 xenograft mouse model

To determine whether HNK can reduce the tumorigenicity in a xenograft model, Kasumi-1 cells were injected subcutaneously into right flank of mice to construct xenograft mouse model. Tumors in HNK-treated mice were significantly smaller than those in control mice (Fig. 7A). Similarly, tumor growth was significantly reduced in HNK-treated mice compared with control mice (Fig. 7B). The average tumor volume in administration of HNK was reduced by 45.7% compared with normal control (Fig. 7C). Also, HNK resulted in 41.2% decrease in average tumor weight (Fig. 7D). Consistent with the results from cell lines, the protein levels of AML1-ETO were significantly decreased but UbcH8 expressions were increased in the tumors obtained from HNK-treated mice in comparison with control mice (Fig. 7E–G).

3.8. Effects of HNK in the C1498 murine AML model

Murine AML cell line C1498 was transfected with a lentivirus encoding enhanced GFP, followed with transfection with MSCV-A/E and named C1498-GFP-MSCV-AE. Western blot demonstrated

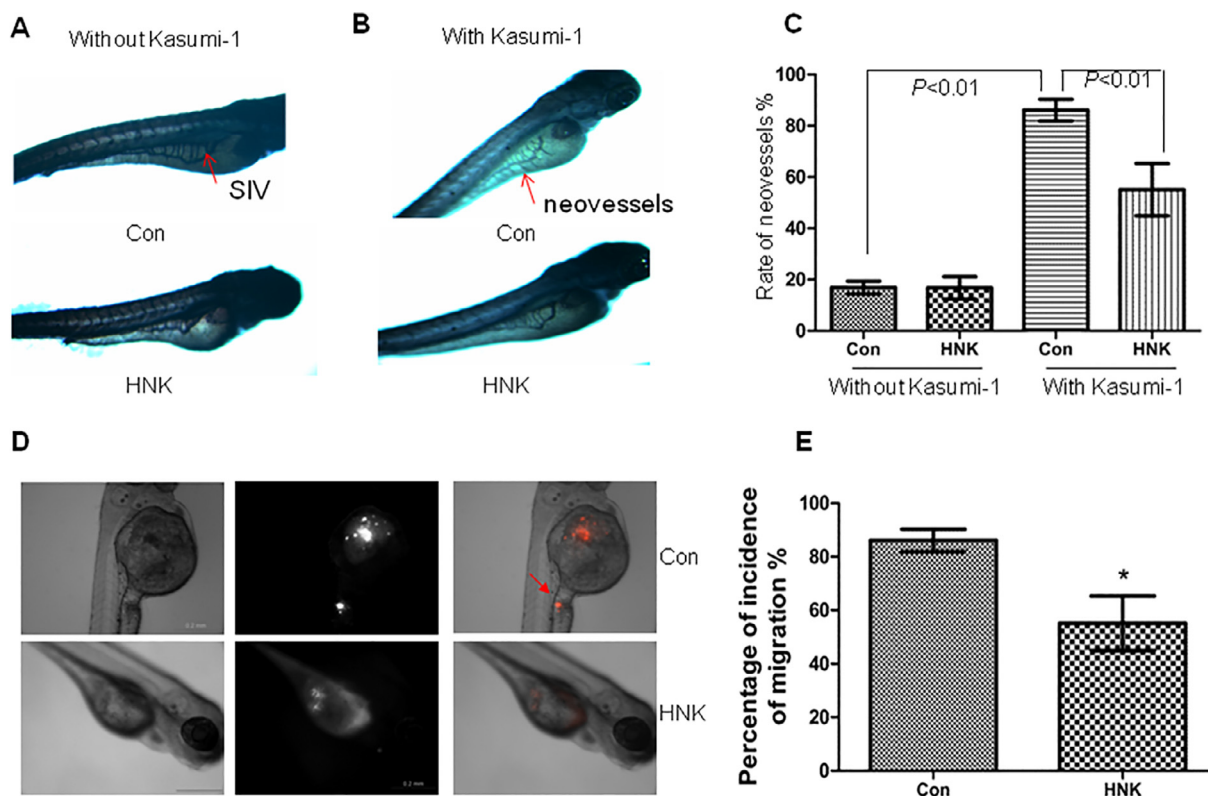


Fig. 6. HNK decreases the angiogenesis and migration in Kasumi-1-injected zebrafishes. Lateral view of embryos stained by alkaline phosphatase at 72 hpf. (A and B) Zebrafishes injected with about 200 Kasumi-1 (B) or without Kasumi-1 cells (A) were treated with 4 μ M HNK for 72 h. The red arrow in Fig. B indicated several neovessels originated from the subintestinal vessels' (SIV) basket. (C) The rates of neovessels were calculated as the numbers of zebrafishes with neovessels against the total numbers of zebrafishes. At least 100 zebrafishes were counted. (D and E) Engraftment of Kasumi-1 cells in zebrafish embryos. Dechorionated embryos were injected with 500 Kasumi-1 cells and examined at day three post-injection (dpi) by contrast phase and fluorescence microscopy. The red arrow indicated the migrated Kasumi-1 cells. * $P < 0.01$ versus untreated fishes. (For interpretation of the references to color in this figure legend, the reader is referred to the web version of this article.)

a significant increase of AML1-ETO protein (Fig. 8A). Similarly, HNK obviously degraded AML1-ETO protein in C1498-GFP-MSCV-A/E cells incubated with 40 μ M HNK for 24 h (Fig. 8B). C1498-GFP-MSCV-A/E cells were intravenously administered in C57/B6 mice to establish murine AML model. The percentage of positive GFP cells from bone marrow in HNK-treated mice was reduced compared with control mice (Fig. 8C and D). Furthermore, Wright's staining morphology indicated that immature blasts were decreased in HNK-treated mice than control mice (Fig. 8E). Also, AML1-ETO protein levels were decreased in HNK-treated mice than control mice (Fig. 8F). Furthermore, we evaluate whether HNK reduced the infiltration of blast cells in spleen. The spleen volume was reduced in mice treated with HNK compared with control mice (Fig. 8G). Extensive infiltrations of immature blast cells destroyed the normal architectures in spleens (Fig. 8H, Left). Accordingly, HNK obviously decreased the infiltrations in HNK-treated mice than control mice (Fig. 8H, Right). Finally, HNK prolonged the survival time by about 26% (median, 15 days for control mice versus 19 days for HNK-treated mice; $P < 0.01$; Fig. 8I).

4. Discussion

AML1-ETO is a key factor for leukemogenesis in AML with t(8;21) and disruption of AML1-ETO protein might facilitate the clinical treatment of AML patients with t(8;21). Here, we discover that a natural compound HNK strongly degrades inducible expression and constitutive expression of AML1-ETO protein through enhancing UbCH8 expression. Intriguingly, HNK-induced degradation of AML1-ETO is independent of active caspase-3. Mechanistically, HNK increases the expression of UbCH8 through enhancing

accumulation of acetylated histones in the promoter of UbCH8. Therefore, HNK might serve as the lead natural compound for the development of AML1-ETO-targeted agent.

Previous data indicated that AML1-ETO was degraded or cleaved in apoptotic condition accompanied with activation of caspase-3. For example, Eriocalyxin B induced caspase-3-dependent apoptosis and degradation of AML1-ETO. Inhibition of caspase-3 activation by Z-DEVD-fmk effectively prevented Eriocalyxin B-induced degradation of AML1-ETO protein [19]. Oridonin, a diterpenoid extracted from medicinal herbs, not only degraded but also cleaved AML1-ETO protein into a catabolic fragment [10]. Preincubation with caspase-3 inhibitor blocked oridonin-triggered cleavage of AML1-ETO [10]. In addition, Lu et al. reported that AML1-ETO protein was cleaved to four fragments of 70, 49, 40 and 25 kDa by activated caspase-3 during apoptosis, suggesting that AML1-ETO is a direct substrate of caspase-3 [20]. All these data suggest that caspase-3 plays an important role in the degradation or cleavage of AML1-ETO. Although HDAC inhibitor depsipeptide induced apoptosis and degradation of AML1-ETO, pan-caspase inhibitor Z-VAD failed to prevent depsipeptide-induced degradation of AML1-ETO [11]. Consistent with this report [11], pan-caspase inhibitor did not block HNK-induced degradation of AML1-ETO. HNK-induced apoptosis was accompanied by activation of caspase-3 in adult T-cell leukemia [33] and B-cell chronic lymphocytic leukemia [28]. However, low concentration of HNK (20 μ M) activated a novel alternative cell death called paraptosis, which is lack of caspase activation and lack of apoptotic morphology in NB4 and K562 cells [29], suggesting that HNK induced cell death more than apoptosis. Our data indicate that HNK-induced cell death is not accompanied with activation of caspase-3. In sum-

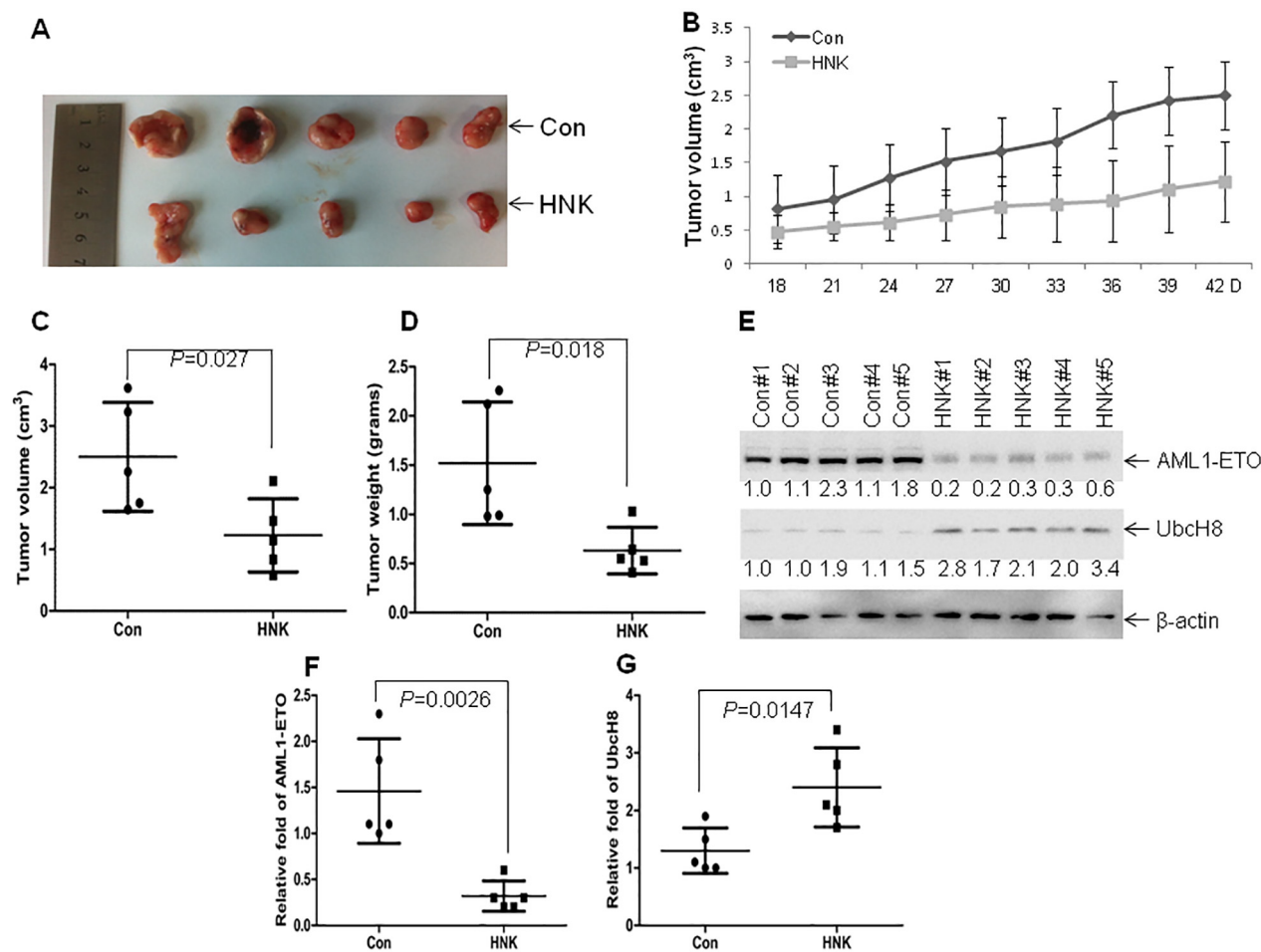


Fig. 7. The anti-tumor effects of HNK in Kasumi-1 tumor xenograft. (A) A photograph of tumors in HNK-treated mice and control mice. (B) Volumes of all tumors were detected every three days after day 18. (C) Volumes of all tumors were measured when the experiment was terminated at day 42 after tumor cell inoculation. (D) Net weights of all tumors were measured at the termination of the experiment. (E) The protein levels of AML1-ETO and Ubch8 were detected in tumor lysates from HNK-treated mice and control mice. The relative intensity of each band after normalization for β -actin is shown under each blot. (F and G) The relative intensity of each band was statistically analyzed. Experiments were repeated three times.

mary, HNK-induced degradation of AML1-ETO in leukemic cells is through ubiquitin-proteasome system but is independent of activation of caspase-3.

AML1-ETO protein was mainly degraded by ubiquitin-proteasome system through Ubch8 and SIAH-1 [26]. We found HNK obviously increased the expression of Ubch8 through triggering the accumulation of acetylated histones in the promoter of Ubch8. Moreover, overexpression of Ubch8 led to the degradation of AML1-ETO and knockdown of Ubch8 by shRNA prevented HNK-induced degradation of AML1-ETO. Because limited expression of Ubch8 might be a prerequisite for stable levels of AML1-ETO and other oncoproteins [26], we speculate that deregulation of Ubch8 might be a step in cellular transformation processes. Protein degradation is a complicated process, which needs hierarchical action of an E1-enzyme, an E2-conjugase and an E3-ligase. There are several E2-conjugases and E3-ligases mediating the degradation of AML1-ETO protein besides Ubch8. We speculate that in steady condition when Ubch8 was knocked down by shRNAs, other E2-conjugases and E3-ligases will play compensatory role to maintain the stable level of AML1-ETO protein. Therefore, decreasing Ubch8 expression could not result in the upregulation of AML1-ETO. Although overexpression of SIAH-1 led to the turnover of AML1-ETO [26], HNK only slightly increased the expression of SIAH-1, suggesting that Ubch8 but not SIAH-1 plays an important role in HNK-

induced degradation of AML1-ETO. Ubch8 might be a potential target for the degradation of AML1-ETO.

HDAC inhibitor VPA increased ubiquitylation of endogenous AML1-ETO and induced degradation of AML1-ETO via upregulation of Ubch8 [26]. Consistent with VPA, our data indicate that another HDAC inhibitor TSA degraded AML1-ETO and increased the expression of Ubch8 in Kasumi-1 cells, suggesting that inhibiting HDAC activities might contribute to the degradation of AML1-ETO. Additionally, HNK failed to alter HSP90 expression, excluding the role of HSP90 in HNK-induced degradation of AML1-ETO. In conclusion, HNK degrades AML1-ETO protein through upregulation of Ubch8 due to the accumulation of acetylated histones in the promoter of Ubch8.

Degrading oncoproteins through enhancing ubiquitin-proteasome activity is a promising method for some oncoproteins, which are deemed to be undruggable. For example, c-Myc or β -catenin is difficult to be directly destroyed by drugs. Degrasyn, a small synthetic molecule, induces proteasomal destruction of c-Myc protein [34]. Docosahexaenoic acid induces proteasome-dependent degradation of β -catenin in human colorectal cancer cells [35]. Furthermore, Lenalidomide (LEN), a clinical drug used for multiple myeloma, induces ubiquitination and degradation of Ikaros family zinc finger proteins 1 and 3 (IKZF1 and IKZF3) through binding and co-opting cereblon E3 ligase [36]. Intriguingly, LEN degrades these two proteins via enhancing the binding activity of cereblon to

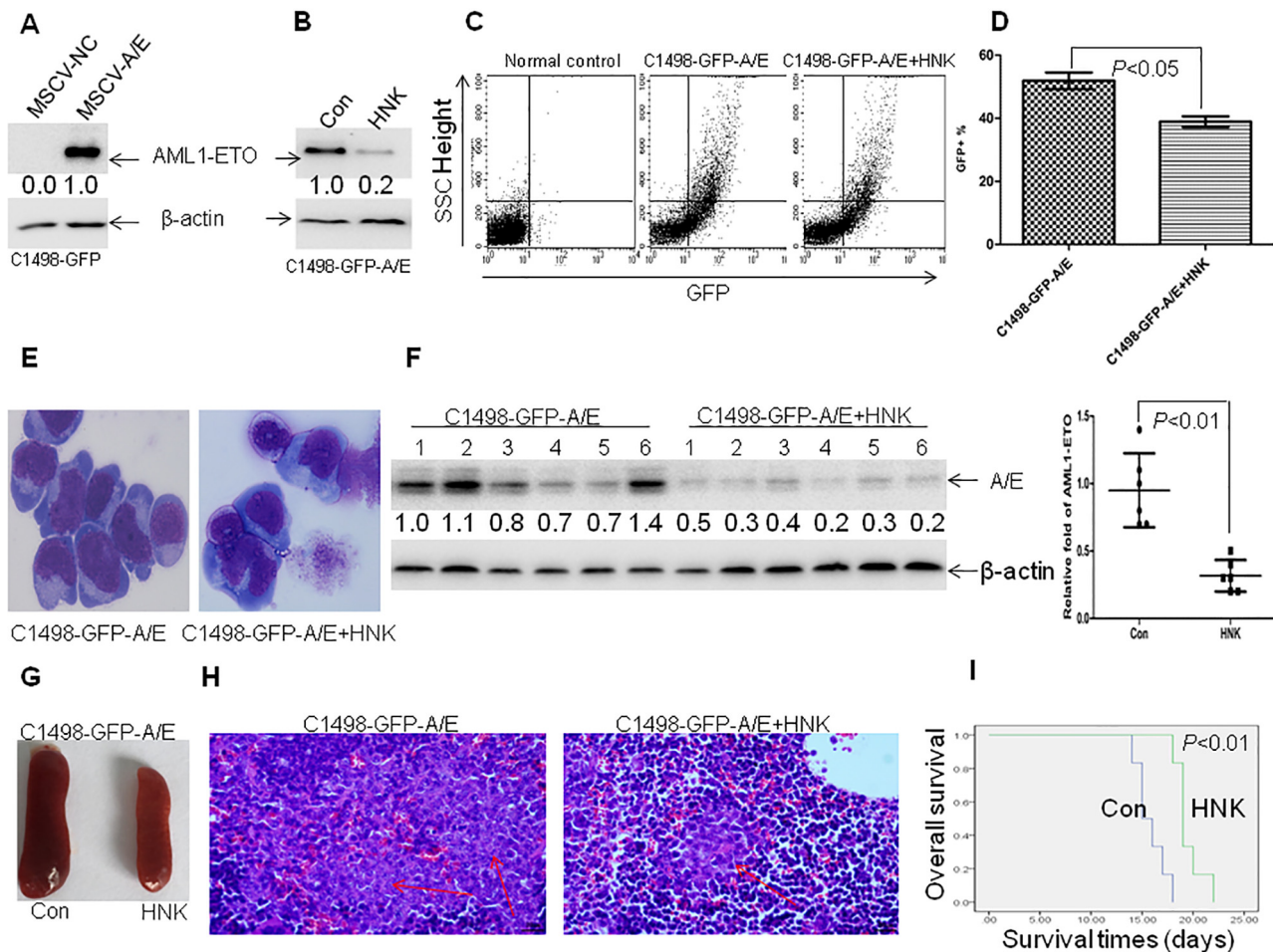


Fig. 8. HNK degrades AML-ETO protein in the C1498 murine AML model. (A) C1498 cells were transfected with lentivirus vector pLVX-IRES-ZsGreen1, followed with selection by flowcytometry. The positive GFP cells are named C1498-GFP cells, which were further transfected with MSCV-A/E and treated with puromycin for one week. Western blot were taken to detect AML1-ETO expression. (B) AML1-ETO expression was measured in C1498-GFP-A/E cells treated with 40 μ M HNK for 24 h. C1498-GFP cells carrying AML1-ETO were called C1498-GFP-A/E. (C and D) Bone marrow mononuclear cells were extracted from mice, which were intravenously injected with C1498-GFP-A/E and treated with HNK or not. GFP-positive cells were analyzed by flowcytometry. BM mononuclear cells from normal B6 mouse are indicated with negative GFP (Fig. 3C left). (E) Bone marrow blast cells were observed by Wright's staining in HNK-treated mice or control mice. (F) AML1-ETO was detected in bone marrow mononuclear cells from HNK-treated mice ($n = 6$) or control mice ($n = 6$) by western blot (Left). The relative intensity of each band after normalization for β -actin is shown under each blot and statistically analyzed (Right). All experiments are repeated at least three times. (G) Representative images of spleens were observed from HNK-treated mice and control mice. (H) HE staining was taken to indicate the infiltration of C1498 leukemic cells in murine spleens. (I) HNK prolonged the overall survival rate in murine C1498 AML model.

IKZF1 and IKZF3, but not increasing the expression of cereblon. In contrast, our results indicate that HNK increased the expression of Ubch8. We speculate that the E2 conjugase activity of Ubch8 is increased by HNK due to upregulated expression of Ubch8. However, whether HNK can bind Ubch8 or affect the binding ability of Ubch8 to its substrates is needed for further study. Collectively, enhancing the expression or activity of E2 conjugase or E3 ligase by chemical or natural compounds might contribute to the degradation of oncoproteins.

While having a higher complete remission rate, up to 70% of AML patients with AML1-ETO will relapse for unknown reasons [37]. Thus, as a possible initiating event in disease pathogenesis, degradation of AML1-ETO could potentially be clinically helpful for the AML patients with t(8;21) translocation. HNK induced growth arrest and apoptosis in Kasumi-1 and U937T cells. It is unlikely that these effects are due solely to inducing the degradation of AML1-ETO protein because HNK can target multiple types of signaling pathway [38]. In fact, knockdown of this fusion protein by siRNA has only modest effects on the viability of Kasumi-1 cells, but allows the cells to be forced to differentiate in response to multiple types of agents [39,40]. However, more effective knockdown

of AML1-ETO by ribozyme-mediated targeting of the fusion protein induces both cellular differentiation and eventually cell death [41]. Thus, HNK might be a potential targeted therapy for AML with t(8;21), because it targets multiple signaling pathways, including degradation of AML1-ETO.

Tumor xenograft model using zebrafish represents a promising alternative model in cancer research, because zebrafish offers many advantages, including amenability to *in vivo* manipulation, ease of experimentation, and convenient drug administration. Recently, zebrafish has been proposed as an alternative to mammalian model to assess the efficacy and toxicity of anti-cancer or -leukemia drugs [42]. We injected Kasumi-1 cells into zebrafish to construct tumor xenograft model and found HNK decreased neovessels originated from the SIV and inhibited migration. Additionally, HNK reduced the tumorigenicity in a xenograft mouse model and prolonged the survival time in the C1498 murine AML model. These studies *in vivo* confirm the degradation of AML1-ETO by HNK and the anti-leukemia activity by HNK. However, the further models such as AML1-ETO knock-in zebrafishes or mice are required to completely evaluate the role of HNK in AML with positive AML1-ETO.

Elimination of the initiating event in leukemogenesis has been proved to be an extremely effective therapeutic strategy. For example, Gleevec for BCR-ABL in CML [43] and ATRA for PML-RAR α in AML with t(15;17) [44] have produced paradigm shifting advances in the treatment of leukemia. However, until now no drugs for specially targeting AML1-ETO fusion protein are used in clinical treatment. Considering that without obvious side effects HNK effectively eliminates AML1-ETO protein, it is possible to enhance the clinical outcome in t(8;21) patients in combination with standard chemotherapeutic approaches.

Competing financial interests

The authors declare that they have no competing commercial or financial interests.

Author contributions

J.F., Z.Q.L. and S.M.G. designed experiments and analyzed results; B.Z. and H.Y.L. performed most of the cellular and molecular experiments; C.Y.X. and H.G.Y. performed animal experiments; J. B.W. partially contributed to biochemical experiments; J.H.F. provided fresh clinical samples; S.M.G. wrote the manuscript. All authors reviewed and approved the manuscript.

Funding

This work was supported by grants from National Natural Science Foundation of China (81501809; 81672087). The key construction academic subject (traditional Chinese medicine) of Zhejiang Province (2012-XK-A28).

Acknowledgments

We thank Prof. Ying Lu (Department of Pathophysiology, Shanghai Jiao Tong University School of Medicine) kindly provides U937-AML1-ETO stable transformant and Prof. Yingli Wu (Department of Pathophysiology, Shanghai Jiao Tong University School of Medicine) kindly provides NSC606985.

References

- [1] S.K. Bohlander, Fusion genes in leukemia: an emerging network, *Cytogenet. Cell Genet.* 91 (2000) 52–56.
- [2] T. Okuda, Z. Cai, S. Yang, N. Lenny, C.J. Lyu, J.M. van Deursen, et al., Expression of a knocked-in AML1-ETO leukemia gene inhibits the establishment of normal definitive hematopoiesis and directly generates dysplastic hematopoietic progenitors, *Blood* 91 (1998) 3134–3143.
- [3] S. Nishida, N. Hosen, T. Shirakata, K. Kanato, M. Yanagihara, S. Nakatsuka, et al., AML1-ETO rapidly induces acute myeloblastic leukemia in cooperation with the Wilms tumor gene, WT1, *Blood* 107 (2006) 3303–3312.
- [4] Y.Y. Wang, L.J. Zhao, C.F. Wu, P. Liu, L. Shi, Y. Liang, et al., C-KIT mutation cooperates with full-length AML1-ETO to induce acute myeloid leukemia in mice, *Proc. Natl. Acad. Sci. U.S.A.* 108 (2011) 2450–2455.
- [5] X.N. Gao, F. Yan, J. Lin, L. Gao, X.L. Lu, S.C. Wei, et al., AML1/ETO cooperates with HIF1 α to promote leukemogenesis through DNMT3a transactivation, *Leukemia* 29 (2015) 1730–1740.
- [6] W. Jin, K. Wu, Y.Z. Li, W.T. Yang, B. Zou, F. Zhang, et al., AML1-ETO targets and suppresses cathepsin G, a serine protease, which is able to degrade AML1-ETO in t(8;21) acute myeloid leukemia, *Oncogene* 32 (2013) 1978–1987.
- [7] B. Linggi, C. Muller-Tidow, L. van de Locht, M. Hu, J. Nip, H. Serve, et al., The t(8;21) fusion protein, AML1 ETO, specifically represses the transcription of the p14(ARF) tumor suppressor in acute myeloid leukemia, *Nat. Med.* 8 (2002) 743–750.
- [8] L.F. Peterson, D.E. Zhang, The 8;21 translocation in leukemogenesis, *Oncogene* 23 (2004) 4255–4262.
- [9] J. Dunne, C. Cullmann, M. Ritter, N.M. Soria, B. Drescher, S. Debernardi, et al., siRNA-mediated AML1/MTG8 depletion affects differentiation and proliferation-associated gene expression in t(8;21)-positive cell lines and primary AML blasts, *Oncogene* 25 (2006) 6067–6078.
- [10] G.B. Zhou, H. Kang, L. Wang, L. Gao, P. Liu, J. Xie, et al., Oridonin, a diterpenoid extracted from medicinal herbs, targets AML1-ETO fusion protein and shows potent antitumor activity with low adverse effects on t(8;21) leukemia in vitro and in vivo, *Blood* 109 (2007) 3441–3450.
- [11] G. Yang, M.A. Thompson, S.J. Brandt, S.W. Hiebert, Histone deacetylase inhibitors induce the degradation of the t(8;21) fusion oncoprotein, *Oncogene* 26 (2007) 91–101.
- [12] G. Chen, J. Izso, Y. Demizu, F. Wang, S. Guha, X. Wu, et al., Different redox states in malignant and nonmalignant esophageal epithelial cells and differential cytotoxic responses to bile acid and honokiol, *Antioxid. Redox Signal.* 11 (2009) 1083–1095.
- [13] D.B. Avtanski, A. Nagalingam, P. Kuppasamy, M.Y. Bonner, J.L. Arbiser, N.K. Saxena, et al., Honokiol abrogates leptin-induced tumor progression by inhibiting Wnt1-MTA1-beta-catenin signaling axis in a microRNA-34a dependent manner, *Oncotargets* 6 (2015) 16396–16410.
- [14] M.K. Pandey, B. Sung, B.B. Aggarwal, Betulinic acid suppresses STAT3 activation pathway through induction of protein tyrosine phosphatase SHP-1 in human multiple myeloma cells, *Int. J. Cancer* 127 (2010) 282–292.
- [15] L. Bi, Z. Yu, J. Wu, K. Yu, G. Hong, Z. Lu, et al., Honokiol inhibits constitutive and inducible STAT3 signaling via PU.1-induced SHP1 expression in acute myeloid leukemia cells, *Tohoku J. Exp. Med.* 237 (2015) 163–172.
- [16] T. Singh, N.A. Gupta, S. Xu, R. Prasad, S.E. Velu, S.K. Katiyar, Honokiol inhibits the growth of head and neck squamous cell carcinoma by targeting epidermal growth factor receptor, *Oncotargets* 6 (2015) 21268–21282.
- [17] Y. Wang, Z. Yang, X. Zhao, Honokiol induces paraptosis and apoptosis and exhibits schedule-dependent synergy in combination with imatinib in human leukemia cells, *Toxicol. Mech. Methods* 20 (2010) 234–241.
- [18] H.Y. Li, H.G. Ye, C.Q. Chen, L.H. Yin, J.B. Wu, L.C. He, et al., Honokiol induces cell cycle arrest and apoptosis via inhibiting class I histone deacetylases in acute myeloid leukemia, *J. Cell. Biochem.* 116 (2015) 287–298.
- [19] L. Wang, W.L. Zhao, J.S. Yan, P. Liu, H.P. Sun, G.B. Zhou, et al., Eriocalyxin B induces apoptosis of t(8;21) leukemia cells through NF-kappaB and MAPK signaling pathways and triggers degradation of AML1-ETO oncoprotein in a caspase-3-dependent manner, *Cell Death Differ.* 14 (2007) 306–317.
- [20] Y. Lu, Z.G. Peng, T.T. Yuan, Q.Q. Yin, L. Xia, G.Q. Chen, Multi-sites cleavage of leukemogenic AML1-ETO fusion protein by caspase-3 and its contribution to increased apoptotic sensitivity, *Leukemia* 22 (2008) 378–386.
- [21] M. Fliegau, M. Stock, T. Berg, M. Lubbert, Williams-Beuren syndrome critical region-5/non-T-cell activation linker: a novel target gene of AML1/ETO, *Oncogene* 23 (2004) 9070–9081.
- [22] E. Beillard, N. Pallisgaard, V.H. van der Velden, W. Bi, R. Dee, E. van der Schoot, et al., Evaluation of candidate control genes for diagnosis and residual disease detection in leukemic patients using ‘real-time’ quantitative reverse-transcriptase polymerase chain reaction (RQ-PCR) – a Europe against cancer program, *Leukemia* 17 (2003) 2474–2486.
- [23] J. Gabert, E. Beillard, V.H. van der Velden, W. Bi, D. Grimwade, N. Pallisgaard, et al., Standardization and quality control studies of ‘real-time’ quantitative reverse transcriptase polymerase chain reaction of fusion gene transcripts for residual disease detection in leukemia – a Europe against cancer program, *Leukemia* 17 (2003) 2318–2357.
- [24] D.B. Avtanski, A. Nagalingam, M.Y. Bonner, J.L. Arbiser, N.K. Saxena, D. Sharma, Honokiol activates LKB1-miR-34a axis and antagonizes the oncogenic actions of leptin in breast cancer, *Oncotargets* 6 (2015) 29947–29962.
- [25] S.A. Serniwa, G.S. Shaw, The structure of the Ubch8-ubiquitin complex shows a unique ubiquitin interaction site, *Biochemistry* 48 (2009) 12169–12179.
- [26] O.H. Kramer, S. Muller, M. Buchwald, S. Reichardt, T. Heinzel, Mechanism for ubiquitylation of the leukemia fusion proteins AML1-ETO and PML-RARalpha, *FASEB J.* 22 (2008) 1369–1379.
- [27] C. Marques, P. Pereira, A. Taylor, J.N. Liang, V.N. Reddy, L.I. Szweda, et al., Ubiquitin-dependent lysosomal degradation of the HNE-modified proteins in lens epithelial cells, *FASEB J.* 18 (2004) 1424–1426.
- [28] T.E. Battle, J. Arbiser, D.A. Frank, The natural product honokiol induces caspase-dependent apoptosis in B-cell chronic lymphocytic leukemia (B-CLL) cells, *Blood* 106 (2005) 690–697.
- [29] Y. Wang, X. Zhu, Z. Yang, X. Zhao, Honokiol induces caspase-independent paraptosis via reactive oxygen species production that is accompanied by apoptosis in leukemia cells, *Biochem. Biophys. Res. Commun.* 430 (2013) 876–882.
- [30] M.L. Torgersen, N. Engedal, S.O. Boe, P. Hokland, A. Simonsen, Targeting autophagy potentiates the apoptotic effect of histone deacetylase inhibitors in t(8;21) AML cells, *Blood* 122 (2013) 2467–2476.
- [31] T. Singh, R. Prasad, S.K. Katiyar, Inhibition of class I histone deacetylases in non-small cell lung cancer by honokiol leads to suppression of cancer cell growth and induction of cell death in vitro and in vivo, *Epigenetics* 8 (2012) 54–65.
- [32] B. Pruvot, A. Jacquel, N. Droin, P. Auberger, D. Bouscary, J. Tamburini, et al., Leukemic cell xenograft in zebrafish embryo for investigating drug efficacy, *Haematologica* 96 (2011) 612–616.
- [33] C. Ishikawa, J.L. Arbiser, N. Mori, Honokiol induces cell cycle arrest and apoptosis via inhibition of survival signals in adult T-cell leukemia, *Biochim. Biophys. Acta* 2012 (2012) 879–887.
- [34] G. Bartholomeusz, M. Talpaz, W. Bornmann, L.Y. Kong, N.J. Donato, Degrasyn activates proteasomal-dependent degradation of c-Myc, *Cancer Res.* 67 (2007) 3912–3918.
- [35] G. Calviello, F. Resci, S. Serini, E. Piccioni, A. Toesca, A. Boninsegna, et al., Docosahexaenoic acid induces proteasome-dependent degradation of beta-catenin, down-regulation of survivin and apoptosis in human colorectal cancer cells not expressing COX-2, *Carcinogenesis* 28 (2007) 1202–1209.

- [36] G. Lu, R.E. Middleton, H. Sun, M. Naniong, C.J. Ott, C.S. Mitsiades, et al., The myeloma drug lenalidomide promotes the cereblon-dependent destruction of Ikaros proteins, *Science* 343 (2014) 305–309.
- [37] P. Paschka, G. Marcucci, A.S. Ruppert, K. Mrozek, H. Chen, R.A. Kittles, et al., Adverse prognostic significance of KIT mutations in adult acute myeloid leukemia with inv(16) and t(8;21): a Cancer and Leukemia Group B Study, *J. Clin. Oncol.* 24 (2006) 3904–3911.
- [38] S. Arora, S. Singh, G.A. Piazza, C.M. Contreras, J. Panyam, A.P. Singh, Honokiol: a novel natural agent for cancer prevention and therapy, *Curr. Mol. Med.* 12 (2012) 1244–1252.
- [39] O. Heidenreich, J. Krauter, H. Riehle, P. Hadwiger, M. John, G. Heil, et al., AML1/MTG8 oncogene suppression by small interfering RNAs supports myeloid differentiation of t(8;21)-positive leukemic cells, *Blood* 101 (2003) 3157–3163.
- [40] K. Kasashima, E. Sakota, T. Kozu, Discrimination of target by siRNA: designing of AML1-MTG8 fusion mRNA-specific siRNA sequences, *Biochimie* 86 (2004) 713–721.
- [41] M. Szyrach, F.E. Munchberg, H. Riehle, A. Nordheim, J. Krauter, S. Nagel, et al., Cleavage of AML1/MTG8 by asymmetric hammerhead ribozymes, *Eur. J. Biochem.* 268 (2001) 3550–3557.
- [42] S. Ridges, W.L. Heaton, D. Joshi, H. Choi, A. Eiring, L. Batchelor, et al., Zebrafish screen identifies novel compound with selective toxicity against leukemia, *Blood* 119 (2012) 5621–5631.
- [43] J. Topaly, W.J. Zeller, S. Fruehauf, Synergistic activity of the new ABL-specific tyrosine kinase inhibitor STI571 and chemotherapeutic drugs on BCR-ABL-positive chronic myelogenous leukemia cells, *Leukemia* 15 (2001) 342–347.
- [44] M.E. Huang, Y.C. Ye, S.R. Chen, J.R. Chai, J.X. Lu, L. Zhao, et al., Use of all-trans retinoic acid in the treatment of acute promyelocytic leukemia, *Blood* 72 (1988) 567–572.